# Small-Angle Neutron Scattering Investigation of Pressure Influence on the Structure of Weakly Charged Poly(*N*-isopropylacrylamide) Solutions and Gels

**Irina Nasimova,† Takeshi Karino, Satoshi Okabe, Michihiro Nagao, and Mitsuhiro Shibayama***

*Neutron Science Laboratory, Institute for Solid State Physics, University of Tokyo, Tokai, Ibaraki 319-1106, Japan*

*Received May 13, 2004; Revised Manuscript Received July 20, 2004*

ABSTRACT: Effects of pressure on the phase separation and structure of weakly charged poly(*N*-isopropylacrylamide-*co*-acrylic acid) (PNIPA−AAc) solutions and gels with 7 wt % were investigated by small-angle neutron scattering (SANS). The phase diagrams were determined in the pressure−temperature ($P-T$) plane for the solution and gel with a light scattering method, which were parabolic functions, having maxima at ($P$ = 38.1 MPa, $T$ = 37.1 °C; for the solution) and (121.6 MPa, 51.6 °C; for the gel). SANS experiments were carried out according to the $P-T$ phase diagrams. At the low temperature and pressure region, where the systems were in one phase, the scattering intensity functions, $I(q)$s, were well described with an Ornstein−Zernike function. However, a scattering maximum appeared in $I(q)$s at elevated temperatures and pressures. The regions where a scattering maximum was observed at $T$ = 45 °C were $P$ < 70 MPa and 200 MPa < $P$ for the gel and $P$ < 70 MPa for the solution. This scattering maximum is due to microphase separation as a result of antagonism between the electrostatic and hydrophobic interactions. In the case of the solution, an upturn in $I(q)$ at the low $q$ region was observed, indicating occurrence of macrophase separation in addition to microphase separation. For the polymer gels, on the other hand, such an upturn in $I(q)$ was not observed as a result of pinning effect of cross-links. The phase behavior and critical phenomena of PNIPA−AAc gels and solutions will be discussed from the viewpoint of pressure effects on the hydrophobic interaction.

## Introduction

Poly(*N*-isopropylacrylamide) (PNIPA) is one of the most well-known thermosensitive polymers that undergo a coil−globule transition in water by increasing temperature.[1,2] The temperature sensitivity of this polymer is ascribed to the hydrophobicity of the *N*-isopropyl groups located on the side chain. At low temperatures (below 32 °C), PNIPA chains are solvated in water owing to "iceberg structure" formation of water surrounding the hydrophobic *N*-isopropyl groups.[3] An increase of temperature leads to melting of the iceberg structure, resulting in aggregation of PNIPA chains. It is known that not only temperature but also (1) an addition of organic solvents such as ethanol or acetone[4] or (2) pressurizing[5−9] can affect the phase behavior of PNIPA−aqueous systems. The pressure sensitivity is ascribed to nonzero volume change of mixing, which is sensitive to the hydrostatic pressure. There are a number of works in which pressure-induced volume phase transitions of PNIPA and weakly charged PNIPA gels were investigated from the macroscopic point of view, such as swelling−shrinking behavior of polymer gels.[7,8,10] At low pressures and temperatures, PNIPA solutions and gels are in one phase, while they undergo phase separation at high temperatures and pressures. Interestingly enough, however, the phase diagram is a parabolic function with a maximum at a certain pressure $P = P_c$ in the pressure−temperature ($P-T$) plane as was reported by Kato,[6,7] Rebelo et al.,[9] and Isono et al.[11]

In one of our recent investigations,[11] pressure-induced phase separation of neutral PNIPA gels and solutions was investigated by small-angle neutron scattering (SANS). It was shown for the solution that scattering intensity function, $I(q)$, was well represented by a Lorentz function (L; an Ornstein−Zernike function) at low temperatures and pressures, where $q$ is the magnitude of the scattering vector. By approaching the phase boundary, the correlation length diverged, from which a spinodal curve was determined. The spinodal curve seemed to merge with the cloud point curve at $P_c$. $I(q)$s for the gel were also well represented by an L-function at low pressures and temperatures. However, $I(q)$s increased much rapidly when approaching the spinodal than that predicted by the L-function and were represented with a sum of L- and squared-Lorentz (SL) functions. This means that cross-link inhomogeneities become dominant near the spinodal.

An introduction of charges to PNIPA solutions and gels drastically changes their phase behavior.[12] Poly(*N*-isopropylacrylamide-*co*-acrylic acid) (PNIPA−AAc) hydrogels undergo a discrete volume phase transition at their transition temperature. As was shown by Shibayama et al.[13,14] for the PNIPA−AAc gels and solutions, the microphase separation took place for weakly charged polymers in a poor solvent. The theoretical prediction of microphase separation for weakly charged polymers in a poor solvent was done by Borue and Erukhimovich[15] and others.[16] For a polymer in a good solvent, both electrostatic and van der Waals interactions are repulsive, resulting in swelling. On the other hand, in a poor solvent region, the polymer−polymer interaction becomes strong and polymer chains start to shrink. However, the shrinking process gives rise to a decrease of translation entropy of counterions

† On leave from Chair of Physics of Polymers and Crystals, Physics Department, Moscow State University, Moscow 119992, Russia.

* To whom correspondence should be addressed.

10.1021/ma049058e CCC: $27.50 
Published on Web 10/22/2004

because of the localization of ions to maintain the electroneutrality. As a result, a microphase separation takes place in the system in order to compromise the antagonistic requirements. Hence, ordered microdomains with polymer-rich regions are formed, which are observed as a scattering peak in $I(q)$.

We are interested in how hydrostatic pressure affects the phase behavior and microphase separation of weakly charged gels. To answer this question, we carried out a SANS study on PNIPA−AAc gels and solutions near the phase separation region. Furthermore, the pressure dependence of hydrophobic interactions, roles of cross-links, and kinetics of microphase formation/annihilation upon pressure jump are extensively discussed.

## Experimental Section

**Samples.** Poly(*N*-isopropylacrylamide-*co*-acrylic acid) (PNIPA−AAc) copolymer gels and the corresponding linear polymer solutions were prepared by redox copolymerization of NIPA and acrylic acid monomers in deuterated water. The ratio of NIPA/AAc molar monomer concentrations was 668 mM/32 mM. NIPA (0.76 g) and AAc (23 mg) monomers together with 4 mg of ammonium persulfate were dissolved in 10 mL of deuterated water. In the case of gel, 13.5 mg of *N*,*N*′-methylenebis(acrylamide) (cross-linker) was added to the solution. After complete dissolution, the prepolymerization solutions were filtered through a 0.45 $\mu$m micropore. After deggasing, 48 $\mu$L of *N*,*N*,*N*′,*N*′-tetramethylethylenediamine was added to initiate polymerization. These samples were prepared in pressure cells at 20 °C. Thus, prepared samples were used both for DLS and SANS measurements without further treatment.

**DLS Measurements.** Dynamic light scattering (DLS) studies were carried out on a static/dynamic compact goniometer (SLS/DLS-5000), ALV, Langen, Germany. A He−Ne laser with a power of 22 mW (wavelength, $\lambda = 6328$ Å) was used as the incident beam. The decay rate distribution functions $G(\Gamma)$ were calculated using the CONTIN data analysis package.[17]

**SANS Measurements.** Pressure-dependent SANS experiments were carried out at SANS-U, owned by the University of Tokyo, placed at the JRR-3M reactor guide hall, the Japan Atomic Energy Research Institute. The wavelength of the neutrons was monochromatized to be 7.0 Å with a velocity selector. The sample-to-detector distances were 8.00, 4.00, and 2.00 m, which provided the experimental $q$ range to be from 0.004 to 0.18 Å$^{-1}$. Pressure-dependent SANS experiments were conducted with a pressure chamber, PCI-400-SANS, Teramex, Co. Ltd., Kyoto, Japan. The PCI-400-SANS is an inner cell-type pressure chamber with sapphire windows, and the pressure can reach 400 MPa. The applied pressure is transmitted via a rubber tube connected to the inner cell made of aluminum with quartz and Ti windows. The sample width was 4 mm. The outer chamber was filled with $D_2O$, and the pressure was controlled by pressurizing $D_2O$ by a double-cylinder hand pump. The SANS measurements were conducted at $T = 25$, 40, and 45 °C. The temperature of the sample was regulated by circulating water from a Neslab RTE-111 thermocontroller with the precision of ±0.1 °C. The scattered neutrons were counted with a two-dimensional position-sensitive detector and circularly averaged. Corrections for air, cell, transmission, and solvent scatterings were made before normalizing to the absolute intensity. For the absolute intensity calibration a polyethylene slab (Lupolen) sample was used. The polyethylene sample was calibrated with the incoherent scattering of vanadium standard. After the absolute intensity calculation, incoherent scattering correction was made by subtraction of the scattering from the corresponding monomer solution.

## Results and Discussion

**1. Phase Diagram.** Figure 1 shows the phase diagrams for PNIPA−AAc solution and gel in $D_2O$ in the $P-T$ plane. The data points for the polymer solution indicate the cloud point curve which was observed with the accuracy of ±0.5 °C by visual observation at the scattering angle of 90°. In the case of PNIPA−AAc gel, on the other hand, determination of cloud points was difficult since the scattering intensity was too low for detection of cloud point. This is due to the fact that cross-links suppress macrophase separation, and a gel sample remains transparent even in a shrunken state.

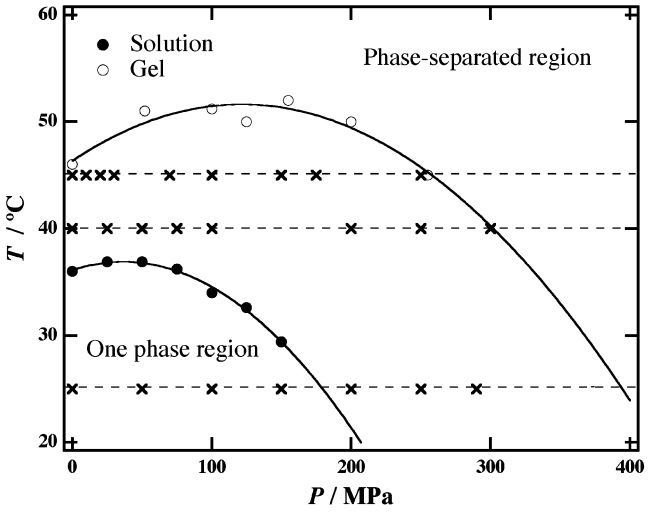


**Figure 1.** Pressure−temperature phase diagrams of PNIPA−AAc (668 mM/32 mM) gel and solution in $D_2O$. The solid lines are drawn by the curve-fitting with parabolic functions. The crosses connected with the dashed lines denote the pressures and temperatures at which SANS experiments were carried out.

The phase separation temperatures and pressures were evaluated by DLS measurements by scanning temperature at which the intensity correlation function, $g^{(2)}(\tau)$, became flat at a given pressure. Figure 2 shows (a) the variations of $g^{(2)}(\tau)$s and (b) the decay rate distribution functions, $G(\Gamma)$s, with temperature at atmospheric pressure (i.e., $P = 0.1$ MPa), where $\tau$ is the time lag and $\Gamma$ is the decay rate. As can be seen from this figure, flattening in $g^{(2)}(\tau)$ and a drastic broadening in $G(\Gamma)$ took place at 44.5 °C with increasing temperature. We conjecture that these temperatures correspond to the microphase separation temperatures at which local chain mobility freezes due to formation of polymer-rich domains and immobilization of polymer chain inside them. Thus, the phase separation temperature was determined as a function of pressure. It should be noted here that $g^{(2)}(\tau)$s for $T \leq 44.5$ °C do not behave systematically with respect to temperature. This is due to the nonergodic nature of gels,[18] meaning that the scattering intensity strongly fluctuates with sampling position. According to Panyukov and Rabin,[19] each subensemble of a gel has a single microscopic equilibrium state under given thermodynamic condition. The nonergodicity of gels appears when one considers different subensembles in a gel. However, the thermodynamics deals with the ensemble of these subensembles by taking the limit of $q$ infinite. This is why macroscopic properties, such as the degree of swelling, are uniquely determined by the thermodynamics of gels. In this work, the phase boundary (at which a flattening takes place in $g^{(2)}(\tau)$) was determined by light scattering. Hence, it requires a certain allowance of the phase boundary region because nonergodicity is involved. Because of the reason given above, the observed curve does not repre-

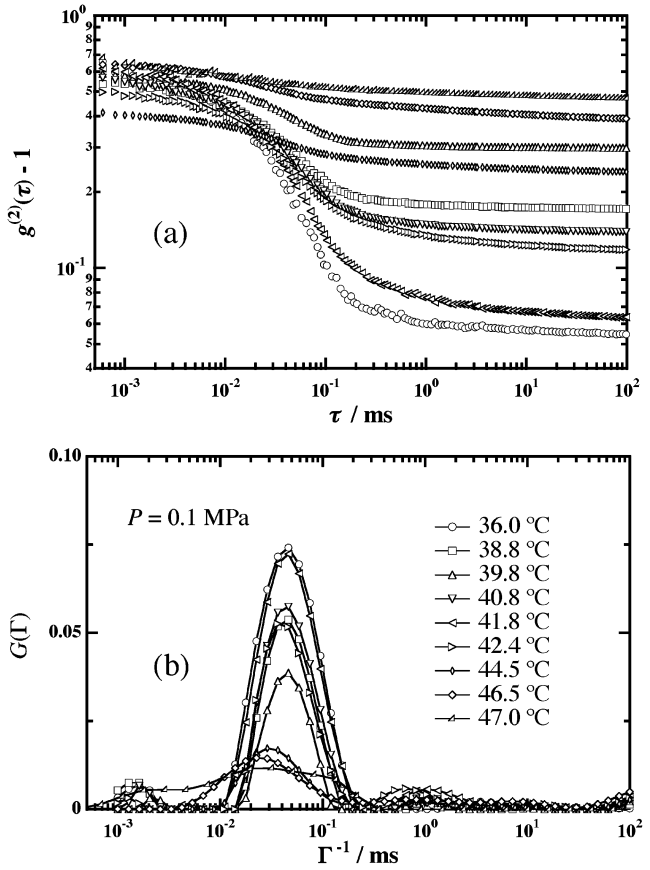


**Figure 2.** Variation of (a) the intensity correlation functions, $g^{(2)}(\tau)$, and (b) the decay rate distribution functions, $G(\Gamma)$, with temperature for PNIPA−AAc gel observed at $P$ = 0.1 MPa. Scattering angle was 90°.

sent the exact phase boundary but gives a guideline about microphase separation.

Similar to the other investigations,[7,9,11,20] it was found that each phase diagram had a maximum. In this case, the phase diagrams were quadratic functions given by

$$T_{\mathrm{soln}} = -7.90 \times 10^{-4}(P_{\mathrm{c}} - 38.1\ [\mathrm{MPa}])^2 + 37.1\ [°\mathrm{C}] \quad (1)$$

$$T_{\mathrm{gel}} = -3.60 \times 10^{-4}(P_{\mathrm{c}} - 121.6\ [\mathrm{MPa}])^2 + 51.6\ [°\mathrm{C}] \quad (2)$$

where the critical pressure, $P_{\mathrm{c}}$, and temperature, $T_{\mathrm{c}}$, were evaluated to be ($P_{\mathrm{c}}$, $T_{\mathrm{c}}$) = (38.1 MPa, 37.1 °C) and (121.6 MPa, 51.6 °C) respectively for the PNIPA−AAc solution and gel. It should be noted that both $P_{\mathrm{c}}$ and $T_{\mathrm{c}}$ for polymer gel are significantly higher than those for the solution. This is due to the presence of the elasticity contribution in the free energy for the gel, which enlarges the one-phase region significantly.

**2. Origin of Convexity in the Phase Diagram.** Here, let us discuss the reason for the convexity of the phase diagram. According to the Clapeyron−Clausius equation, the derivative of pressure with respect to temperature for the hydrophobic solvation is given by

$$\frac{\mathrm{d}P}{\mathrm{d}T} = \frac{\Delta H_{\mathrm{m}}}{T\Delta \bar{V}_{\mathrm{m}}} \quad (3)$$

where $\Delta H_{\mathrm{m}}$ and $\Delta \bar{V}_{\mathrm{m}}$ are the changes of enthalpy and molar volume by mixing, i.e., hydrophobic solvation, respectively. The values of $\Delta \bar{V}_{\mathrm{m}}$ at atmospheric pressure were measured by Kato[7] to be $\Delta \bar{V}_{\mathrm{m}} = -2.4$ and $-2.7$ cm$^3$/mol for the PNIPA and ionized PNIPA gels, respectively. Thus, at low pressure, while $\Delta \bar{V}_{\mathrm{m}}$ remains negative, pressurizing pushes the phase separation temperature to the higher temperature region.

It should be noted that $\Delta \bar{V}_{\mathrm{m}}$ is a function of pressure, $\Delta \bar{V}_{\mathrm{m}} \equiv \Delta \bar{V}_{\mathrm{m}}(P)$, and a further increase of pressure to $P > P_{\mathrm{c}}$ results in a negative-to-positive change in $\Delta \bar{V}_{\mathrm{m}}$. The scheme that explains the pressure effect on $\Delta \bar{V}_{\mathrm{m}}$ is schematically drawn in Figure 3. Suppose that we have two boxes of the same volume filled with stones (box 1) and fine sand (box 2). By mixing the two, one expects a negative change of mixing volume, $\Delta \bar{V}_{\mathrm{m}}$, since the fine sand can fill the voids among stones. The voids can be

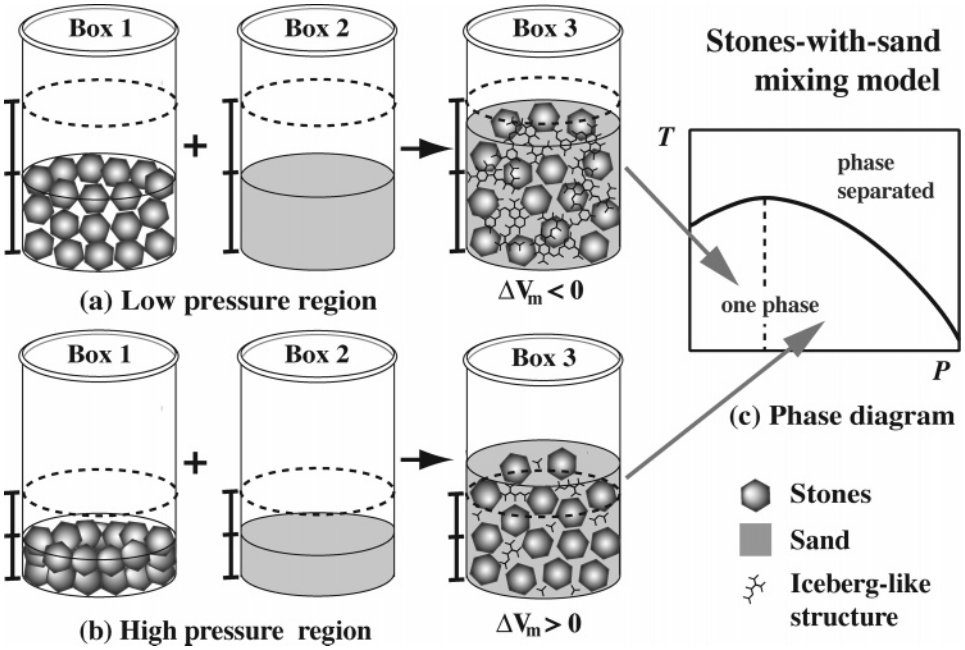


**Figure 3.** Stones-and-sand mixing model explaining the origin of the convexity of the $P$−$T$ phase diagram observed in PNIPA−AAc solution and gel: (a) mixing at low pressure where the stones have large porosity, (b) mixing at high pressures where the stones have small or no porosity, and (c) phase diagram.

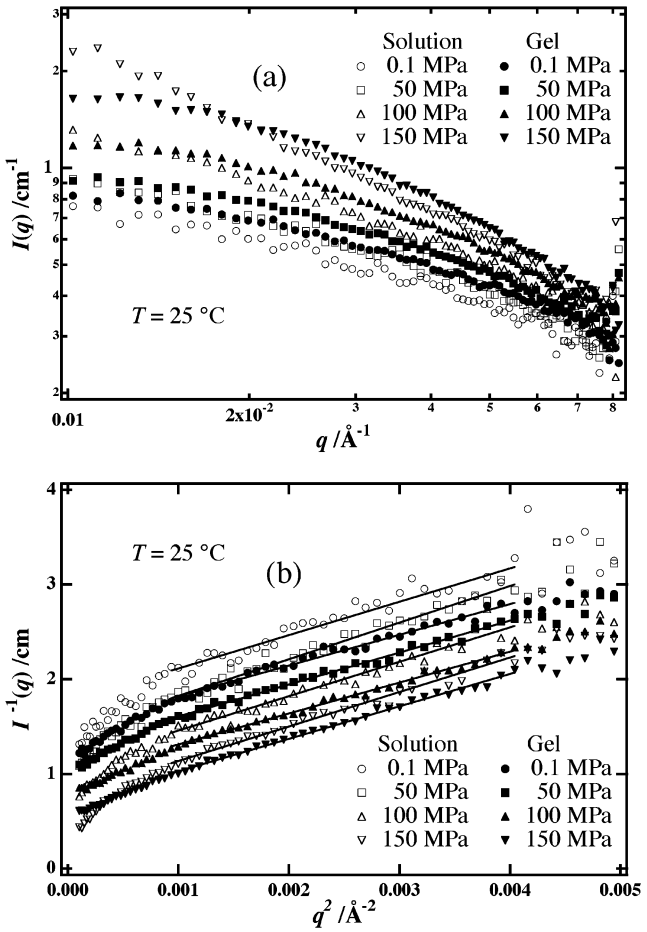


**Figure 4.** (a) Double-logarithmic plot of SANS intensity functions, $I(q)$s, vs scattering vector, $q$, and (b) Ornstein−Zernike (OZ) plot, i.e., $1/I(q)$ vs $q^2$ for PNIPA−AAc gel and solution obtained at various pressures and at $T = 25$ °C. The solid lines represent the fitting results with the OZ function.

regarded as the free volume of the stone (PNIPA). If this free volume is large enough, we still expect a negative value of $\Delta\bar{V}_m$ after "iceberg-like structure formation" of the "sand" (water molecules). However, since the free volume of the stones decreases with increasing pressure as in the case of benzene and some others,[21] the system eventually reaches a point with $\Delta\bar{V}_m = 0$. Since the iceberg formation always accompanies a positive change in volume, the sign of $\Delta\bar{V}_m$ switches from negative to positive above this point. This is why the sign of $dP/dT$ and hence $dT/dP$ becomes negative. Hence, the convexity in the phase diagram is directly related to the change of the sign of $\Delta\bar{V}_m$ since $T$ and $\Delta H_m$ are always positive and negative, respectively.

Using this equation and the value of $\Delta\bar{V}_m$ at the atmospheric condition, we evaluated the value of $\Delta H_m$ to be −5.9 kJ/mol as was done by Kato.[7] This value is close enough to the value reported by Kato ($\Delta H_m = -5.2$ kJ/mol)[7] and of $\Delta H_m$ estimated by DSC measurements (≈2.1−3.5 kJ/mol).[22] Note that the heat of desolvation, i.e., $-\Delta H_m$, is usually measured during a heating process and is endothermic. This corresponds to a melting of "iceberg structure". The negative sign of $\Delta H_m$ means that the solvation process is exothermic and is favorable of mixing.

Otake et al.[23] measured the specific volume of PNIPA aqueous solutions as a function of temperature and pressure and obtained the specific volume ratio (SVR), i.e., the ratio of the specific volume normalized to the specific volume of pure water. Interestingly, SVR is less and larger than unity in one phase and in two phase, respectively, at atmospheric pressure. This experimental observation supports our conjecture. Although they did not observe any significant change in SVR with pressure, we believe that the pressure dependence of the phase diagram for PNIPA aqueous solutions and gels can be explained with this framework.

**3. Temperature and Pressure Dependence of Scattering Profiles. (a) Low-Temperature Region.** Figure 4a presents the variations of scattering intensity profiles at various pressures, $I(q)$s, for PNIPA−AAc gel and solution at $T = 25$ °C, where $q$ is the magnitude of the scattering vector. $I(q)$s are decreasing functions of $q$ and increase with increasing pressure. At atmospheric pressure, when both gel and solution are far from the phase separation point, the scattering functions are more or less superimposed to each other. This means that the gel behaves like a semidilute polymer solution, and the presence of cross-links does not affect the scattering intensity. So, the static inhomogeneities, usually observed in gel systems,[24] are suppressed in the case of charged PNIPA−AAc gel. It is known that the scattered intensity of polymer gels depends on the degree of ionization of the pregel solution in the state of preparation.[25] The polymerization was carried out at pH ≈ 7.7−8.1 where the acrylic acid was ionized. Hence, electrostatic repulsions, present in the solution from the beginning of polymerization, suppress density fluctuations and result in a more homogeneous network. Note that inhomogeneities in a gel in a confined space can be significantly reduced by strong osmotic pressure generating by counterions of the charges. On the other hand, nonergodicity appears when the system loses translational mobility, e.g., by gelation.

Figure 4b shows the Ornstein−Zernike (OZ) plots, i.e., $1/I(q)$ vs $q^2$, for PNIPA−AAc gel and solution at $T = 25$ °C. The solid lines are the fits with Lorentz (or Ornstein−Zernike) function given by

$$I(q) = \frac{I(0)}{1 + \xi^2 q^2} \tag{4}$$

where $\xi$ is the correlation length, i.e., the size of the blobs at polymer chains.[26] The function fits seem to be satisfactory except for the low $q$ regions. These deviations may be due to nonrelaxed concentration fluctuations during polymerization as are often observed for high molecular weight PNIPA solutions prepared by redox polymerization.[27]

The variations of $\xi$ with pressure are presented in Figure 5. It can be seen that the presence of cross-links does not affect the local structure of the PNIPA. The correlation length was also estimated with dynamic light scattering with

$$\xi \approx \frac{kT}{6\pi\eta D} \tag{5}$$

where $\eta$ is the solvent viscosity and $D$ is the collective diffusion coefficient. The value was about 30 Å at the atmospheric pressure (the calculation was made taking into account the difference between the viscosity of $H_2O$ and $D_2O$).[28] This is about twice of the value observed from SANS data. Difference in the correlation lengths evaluated by SANS and DLS is frequently reported, e.g., in the work by Szydlowski at el.[29] for correlation lengths of polystyrene in methylcyclohexane solutions. This is

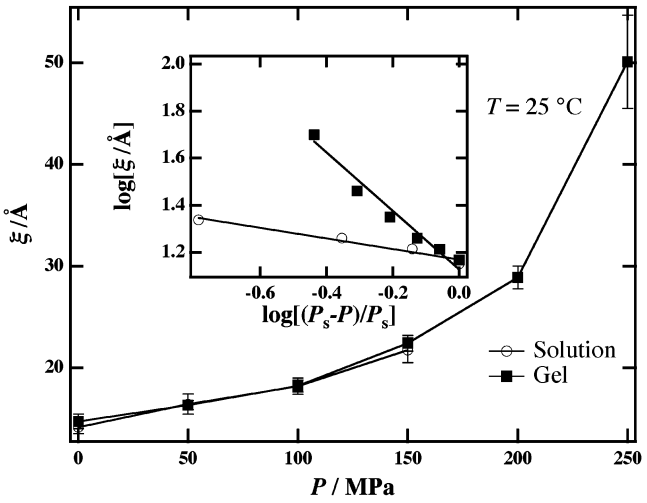


**Figure 5.** Pressure dependence of the correlation length, $\xi$, for PNIPA−AAc gel and solution obtained at $T = 25$ °C. The inset shows a log−log plot of $\xi$ vs $(P_s - P)/P_s$.

due to the employment of the following equation[26] in a DLS analysis with a proportional constant being unity. By taking account these facts, we can conclude that the agreement is successful.

The correlation length increases with increase of pressure as shown in the figure. The inset shows the log−log plots for $\xi$ vs $(P_s - P)/P_s$, where $P_s$ is the spinodal pressure. The plots seem to fall on straight lines, from which a critical exponent, $\nu_P$, was evaluated with the following equation:

$$\xi = \xi_0 |P - P_s|^{-\nu_P} \tag{6}$$

$\nu_P = 1.24$ for the gel and 0.22 for the solution. These numbers are noticeably different from those for noncharged gels and solutions,[11] respectively. We will discuss this issue in a forthcoming paper.[30]

**(b) High-Temperature Region.** The variation of scattering intensity profiles of the PNIPA−AAc gels and solutions with pressure at $T = 40$ and 45 °C are presented in Figure 6a,b. Note that a scattering maximum appears in $I(q)$ for the solution at $(P, T) = (0.1$ MPa, 40 °C), (0.1 MPa, 45 °C), and (30 MPa, 45 °C). On the other hand, for the gel at low pressure the scattering maximum was observed only at $T = 45$ °C. As was discussed in the Introduction, the occurrence of the peak is explained by strong concentration fluctuations that appeared with increasing temperature originating from competition among the electrostatic repulsive interactions, loss of the entropy of counterions, and hydrophobic attractive interaction. As a result, a microphase separation takes place. In the case of polymer solution, an increase of pressure leads to a decrease of maximum intensity, and the scattering peak disappeared for $P \geq 70$ MPa. A further increase of pressure leads to a sharp upturn of $I(q)$ in the low $q$ region. This behavior is significantly different from the gel. In the case of gel for any pressure, there are no upturn in $I(q)$. This divergence in $I(q)$ in the case of polymer solution is due to macrophase separation. An addition of cross-links suppresses the macrophase separation and lowers $I(q)$ in the low $q$ region.

The above experimental evidence may raise a question about the role of cross-links on inhomogeneities of gels. According to Schosseler and co-workers,[31] $I(q)$ for a gel is usually larger than for the corresponding

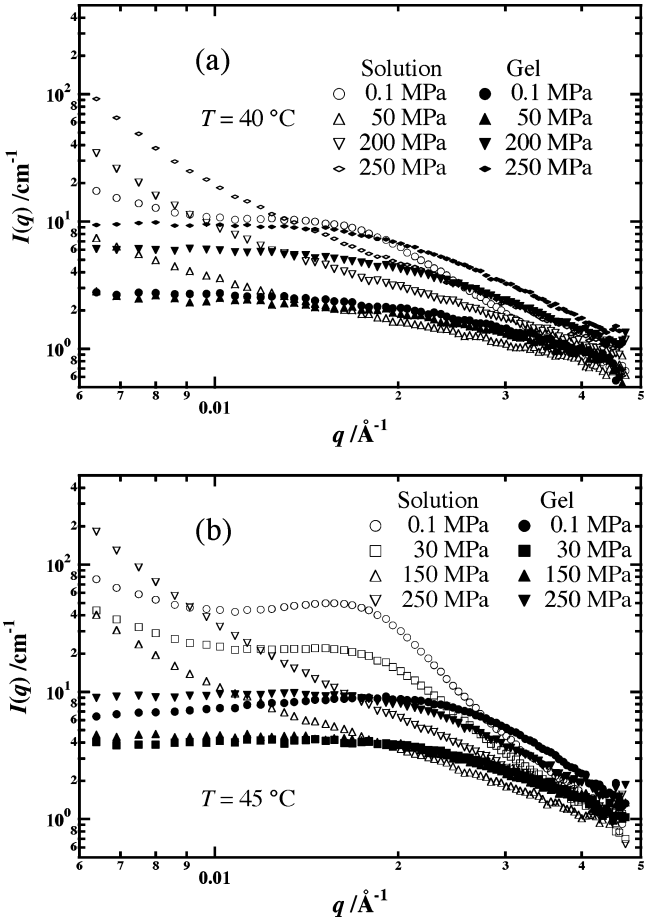


**Figure 6.** Double-logarithmic plot of SANS intensity functions, $I(q)$s, for PNIPA−AAc gel (filled symbols) and solution (open symbols) obtained at various pressures and at (a) $T =$ 40 and (b) 45 °C.

polymer solution as in the case of AAc weakly ionized gels and solutions. The experimental results disclosed in this work are contradictory to the literature. However, it should be noted that our system is not at preparation conditions but is close to a phase separation region. As was discussed by Ikkai et al.,[32] $I(q)$ of a gel is governed by the competition between two opposite effects of cross-linking, i.e., frozen inhomogeneities and pinning. (1) At low temperatures, $I(q)$ is governed by frozen inhomogeneities introduced by cross-link formation. In this case $I_{gel}(q)$ is larger than $I_{sol}(q)$, where $I_{gel}(q)$ and $I_{sol}(q)$ denote the scattering function for gel and sol, respectively. (2) Although a phase separation is expected at high temperature, it is suppressed by a pinning effect of the cross-links. This leads to a suppression of $I(q)$. Hence, $I_{gel}(q) < I_{sol}(q)$.

**(c) Kinetics.** It is well-known that the volume phase transitions of thermosensitive polymers depend on the way in which the condition was changed.[33,34] For example, Shibayama et al.[34] showed that it takes hours to reach a new equilibrium by temperature jump for a gel in equilibrium with water (isobar gel) but not for a deswollen gel (isochore gel). This experiment indicates that an isochore gel can reach a new equilibrium by only changing its local structure without changing its overall volume. In general, the equilibration time after temperature jump depends on the cooperative diffusion coefficient, and the time required for volume change is proportional to the square of the size of the gel. In the case of a pressure experiment, the external conditions

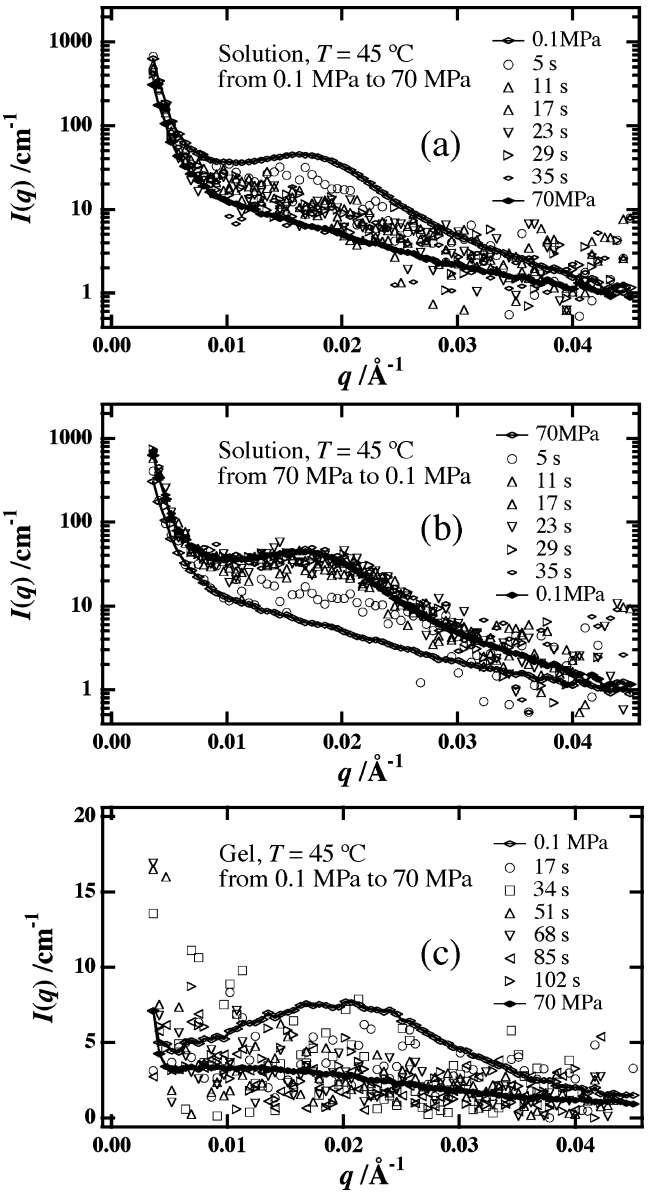


**Figure 7.** Variation of $I(q)$s for PNIPA−AAc solution with time after pressure jump: (a) pressurizing from 0.1 to 70 MPa and (b) depressurizing from 70 to 0.1 MPa; (c) variation of $I(q)$s for PNIPA−AAc gel with time after pressure jump from 0.1 to 70 MPa. The temperature was $T$ = 45 °C. The lines with marks represent the scattering profiles measured for 30 min after 30 min equilibration at a fixed pressure.

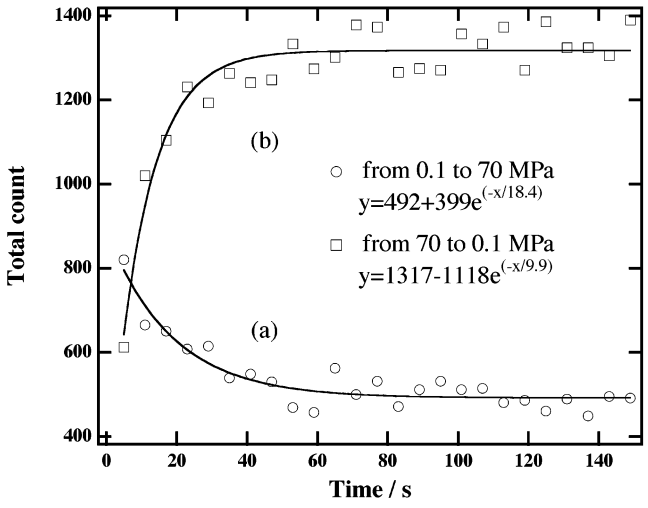


**Figure 8.** Variation of the total scattering intensity for PNIPA-AAc solution collected with the two-dimensional detector for every 5 s as a function of time after (a) pressurizing from 0.1 to 70 MPa and (b) depressurizing from 70 to 0.1 MPa. The solid lines are drawn by curve-fitting with exponential functions.

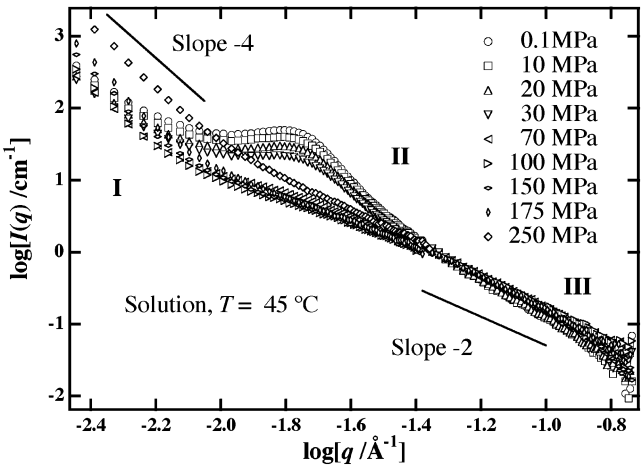


**Figure 9.** Log−log plots of $I(q)$s for PNIPA−AAc solution obtained at various pressures at $T$ = 45 °C. $I(q)$s were obtained with two sample-to-detector distances (SDD), i.e., 8 and 2 m, and then a master curve was constructed. The scattering regions were classified to I (low $q$), II (intermediate $q$), and III (high $q$) regions.

can be changed instantly, and the equilibration time should not depend on the rate of the diffusion. To examine the rate of structure relaxation upon pressure change, we collected the scattering intensity data every 5 s after a jumpwise increase/decrease of pressure and compared the data with scattering profiles measured for the samples held at certain pressure for 30 min.

Figure 7 presents the variation of $I(q)$s with time for PNIPA−AAc solution (a, b) and gel (c) in $D_2O$ at $T$ = 45 °C after pressure jump from 0.1 to 70 MPa (a, c) and from 70 to 0.1 MPa (b). As it can be seen from this figure, structure change occurs during the first 5 s after pressure jump both for the cases of pressurizing (a) and depressurizing (b). The structure change is more clearly observed in the solution since the scattering intensity of the solution is much higher than that of the gel due to the macrophase separation in addition to microphase separation. In the case of the gel, on the other hand, though the scattering intensity is too low to obtain sufficient statistics for such a short measuring time, the difference between 0.1 and 70 MPa is clear, and structure relaxation seems to occur as quickly as in the case of the solution.

Figure 8 shows the variation of the scattering intensity of the solution expressed in total counts as a function of time. As shown in the figure, the variation can be well fitted with a single-exponential function with a relaxation time of $\tau_{jump}$ being roughly 18 and 10 s respectively for the pressuring and depressurizing jump. Hence, we can conclude that a structure relaxation process by pressure jump is very fast and reversible.

**(d) Micro- and Macrophase Separation.** Let us now examine the scattering profiles of the PNIPA−AAc solution obtained at various pressures in more detail. For this purpose, SANS measurements for the PNIPA−AAc solution were carried out with the sample-to-detector distances being 8 and 2 m. This allowed us to

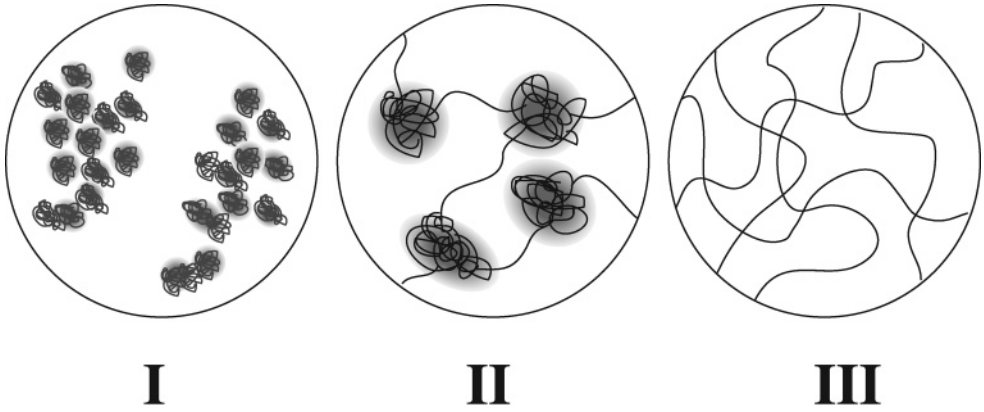


**Figure 10.** Schematic representation explaining the relationship among the three $q$ regions. (I) The low $q$ region where two-phase structure due to the presence of inhomogeneities is preferentially observed, (II) the intermediate $q$ region where both the inhomogeneities and microphase separation are observed, and (III) the high $q$ region where the local chain structures are exclusively observed.

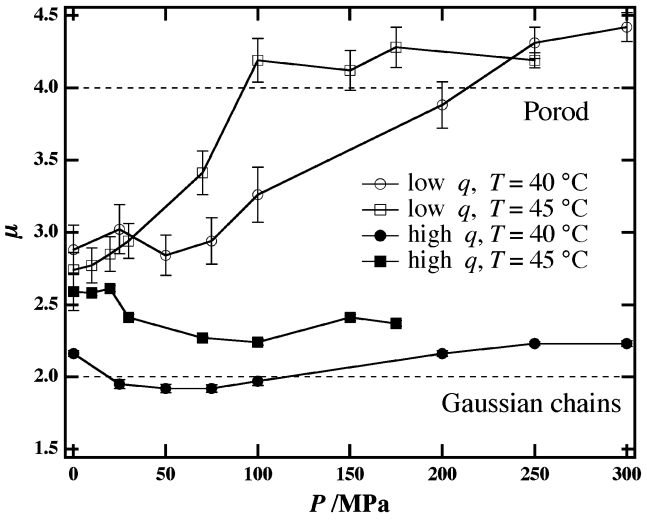


**Figure 11.** Pressure dependence of the scattering exponent $\mu$ for the PNIPA−AAc solution at $T = 40$ and 45 °C. The dashed lines indicate the cases where the Porod law ($\mu = 4$; upper) and the scattering function for semidilute polymer solutions ($\mu = 2$; lower) apply.

observe the experimental $q$ range from 0.004 to 0.18 Å$^{-1}$. Figure 9 presents the variations of scattering intensity profiles. The scattering profiles can be divided into three regions: the low (I) ($\log [q/\text{Å}^{-1}] < -2.1$), the intermediate (II) ($-2.1 \leq \log [q/\text{Å}^{-1}] \leq -1.4$), and the high (III) $q$ regions ($-1.4 \leq \log [q/\text{Å}^{-1}]$). Region I provides the information about the spatial inhomogeneities and is sensitive to macrophase separation. The intermediate II region is related to microphase separation, and the high $q$ region III corresponds to the local structure. The relationship among these regions is schematically drawn in Figure 10, where inhomogeneities are depicted as domains (shade).

The asymptotic behavior of the scattering intensity can be describe by

$$I(q) \sim q^{-\mu} \tag{7}$$

Figure 11 presents the variation of scattering exponent $\mu$, estimated for the low (I) and high (III) $q$ regions, with pressure for $T = 40$ and 45 °C. The dashed lines denote the $\mu$ values for a two-phase system (i.e., the Porod region ($\mu = 4$)[35,36]) and for the Gaussain chains ($\mu = 2$). At the high $q$ region, the scattering exponent is about 2 irrespective of pressure and temperature. At the low $q$ region, on the other hand, the value of the scattering exponent increases from 3 to 4 for $P > 100$ MPa. This behavior means that pressure does not affect the system on the scale of local chains and polymer chains behave like Gaussian chains. On the other hand, pressurizing induces a macrophase separation on the macroscopic scale. According to Figure 9, microphase separation is more pronounced at the low-pressure region ($P < 70$ MPa). An increase of pressure (up to 70 MPa) led to suppression of the phase separation, and the peak disappeared. Further increase of pressure led to an increase of scattering intensity at a lower $q$ region. The increase of scattering exponent from 3 to 4 indicates the growth of a two-phase structure (Porod low), i.e., macrophase separation. The same power law was also observed by Hirokawa et al. in PNIPA gels prepared in a phase-separated region.[37] The deviation from the Porod law in II and III regions is due to the scattering from the matrix which consists of polymer chains in semidilute regime. The iceberg structure may be broken due to pressurizing, resulting in macrophase separation. Pressure dependence of the dielectric constant might be another reason for the intensity upturn by pressurizing. Phillippova et al. discussed the importance of the dielectric constant for microphase separation with ion pairs formation of charged units of polymer for the case of mixed solvents.[38] According to Helgeson and Kirkham,[39] the dielectric constant, $\epsilon$, of water does not change significantly in this pressure region ($\epsilon = 78$ at $P = 0.1$ MPa to 85 at $P \approx 250$ MPa at $T = 25$ °C). However, it is deduced that the dielectric constant of water in the presence of hydrophobic substances is different from that in bulk, and the former may govern the structure factor and the miscibility of PNIPA−AAc. Hence, we concluded that the interesting pressure dependence of $I(q)$ may be ascribed to the pressure dependence of the local $\epsilon$ as well as to the pressure dependence of the interaction parameter.

This observation of micro- and macrophase separations at the low and high pressure regions, respectively, is consistent with macroscopic swelling/shrinking observation. Kato observed that an ionized PNIPA gel underwent two volume-phase transitions at 38.5 °C with increase of pressure.[6] The first one was a discontinuous transition from a shrunken to swollen states at $P \approx 20$ MPa, and the second was a gradual transition from a

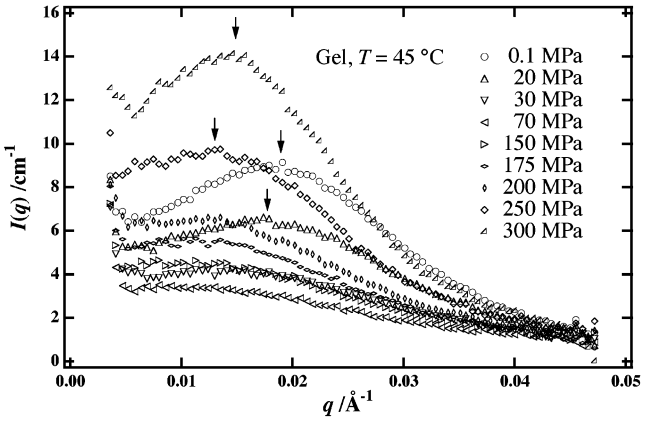


**Figure 12.** Variation of of $I(q)$s for PNIPA−AAc gel with pressure at $T = 45$ °C. The arrows indicate the position of the scattering maximum.

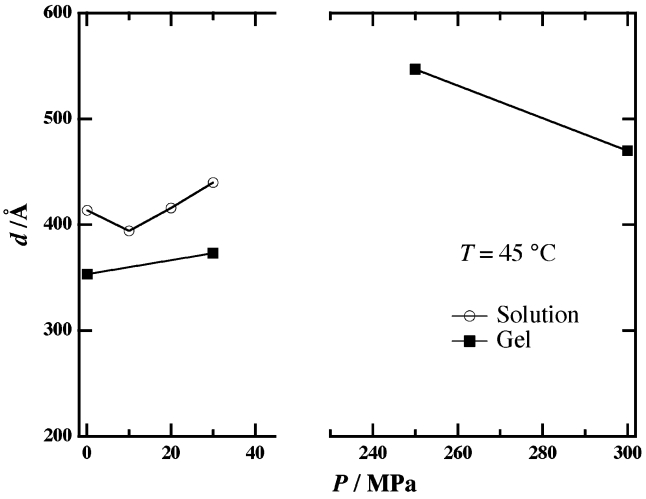


**Figure 13.** Plots of the periodicity of concentration fluctuations, $d$ ($d = 2\pi/q_{max}$), vs pressure for PNIPA−AAc gel and solution at $T = 45$ °C.

swollen to shrunken states for $P \geq 70$ MPa. This means that at high pressures the ionized PNIPA gel behaves similar to a noncharged gel undergoing a continuous transition to a shrunken state.

Figure 12 shows the variations of $I(q)$s for the gel with increase of pressure at $T = 45$ °C. It can be noted that at the beginning, i.e., at the ambient pressure ($P = 0.1$ MPa), a clear scattering maximum, $q_{max}$, responsible for microphase separation is observed in $I(q)$. With increasing pressure, however, the maximum diminishes, similar to the case of the polymer solution, and completely disappears at $P = 70$ MPa. Further increase in $P$ higher than 200 MPa leads to reappearance of scattering maximum but at a lower $q$ value. The appearance of scattering maximum at high pressures at the same $q$ region was also observed at $T = 40$ °C though it was not observed at low pressures.

In Figure 13 are shown the pressure dependences of the long spacing of concentration fluctuations, $d$, given by $d = 2\pi/q_{max}$ for the solution and the gel. This figure indicates that in the case of the gel microphase separation disappears and reappears with a larger periodicity without accompanying macrophase separation. It is needless to mention that a macrophase separation is suppressed due to the pinning effect in a gel. On the other hand, microphase separation exists only at low pressures (i.e., $P \leq 70$ MPa) for the polymer solution. This may be due to the fact that capability of conformation change in the polymer solution allows rearrangement of charges on the polymer chain so as to minimize the free energy increase due to an increase in the hydrophobic interaction. Such rearrangement cannot be attained in the polymer gels due to the presence of cross-links.

The origin of the appearance of the scattering maximum was discussed theoretically by Borue and Erukhimovich[15] and by Rabin and Panyukov.[25] According to these theories proposed by them and experimental studies by Shibayama et al.,[13,27,32] the peak position is a complicated function of the degree of ionization, the interaction parameter (temperature), the polymer volume fraction, and the degree of cross-link. Howerver, none of these studies take into account the effect of pressure. At this stage, it is not clear the reason why the peak shifts to a lower $q$ region at high pressures. We deduce that this shift is due to a significant change in the interaction parameter as well as in the local dielectric constant between $P < P_c$ and $P > P_c$. We will report the pressure effect on the peak position in a forthcoming paper.[30]

## Conclusions

The microstructure and phase separation of weakly charged PNIPA−AAc solutions and gels were investigated as a function of hydrostatic pressure, $P$, and temperature, $T$, by SANS. It was shown that PNIPA−AAc gels and solutions have a convex-upward phase diagram in the pressure−temperature ($P$−$T$) plane. The transition temperature of PNIPA−AAc gels was higher than that of the polymer solutions for any pressure. At low temperature and pressure regions, $I(q)$s for both the gels and solutions are well represented with an Ornstein−Zernike scattering functions. However, $I(q)$s start to deviate from this function as pressure and temperature approach the phase separation curve. The correlation lengths observed at low temperature and pressure regions were almost the same and were increasing function with pressure, indicating absence of cross-linking effect on the structure factor.

At temperatures higher than the cloud point temperature for the solution, a scattering maximum appeared in $I(q)$s at atmospheric pressure. The appearance of the peak indicates that the system undergoes microphase separation. A comparison of the scattering profiles for the gel and solution elucidated the essential roles of cross-links. In the case of polymer solution, macrophase separation takes place together with microphase separation at the low-pressure region. However, an increase of pressure higher than 70 MPa led to suppression of microphase separation due to lowering a gain of the free energy originated from a negative volume change and destruction of iceberg-like structure of water molecules. As a result, the system undergoes macrophase separation with larger inhomogeneities. In the polymer gels, on the other hand, no macrophase separation was observed due to pinning effect of cross-links. The increase of pressure up to 200 MPa led to reappearing of scattering maximum but at a lower $q$, indicating formation of microphase separation with larger periodicity.

**Acknowledgment.** This work is partially supported by the Ministry of Education, Science, Sports and Culture, Japan (Grant-in-Aid and 14350493, 14045216

to M.S.). The SANS experiment was performed with the approval of Institute for Solid State Physics, The University of Tokyo (Proposal No. 03-3503 and 04-4525), at the Japan Atomic Energy Research Institute, Tokai, Japan.

## References and Notes

(1) Shibayama, M.; Tanaka, T. *Adv. Polym. Sci.* **1993**, *109*, 1.
(2) Hirokawa, Y.; Tanaka, T. *J. Chem. Phys.* **1984**, *81*, 6379.
(3) Tanford, C. *Physical Chemistry of Macromolecules*; Wiley: New York, 1961.
(4) Tanaka, T.; Fillmore, D. J.; Sun, S. T.; Nishio, I.; Swislow, G.; Shah, A. *Phys. Rev. Lett.* **1980**, *45*, 1636.
(5) Kato, E. *J. Chem. Phys.* **2000**, *113*, 1310.
(6) Kato, E. *J. Chem. Phys.* **1997**, *106*, 3792.
(7) Kato, E. *J. Appl. Polym. Sci.*, submitted for publication.
(8) Nakamoto, C.; Kitada, T.; Kato, E. *Polym. Gels Networks* **1996**, *4*, 17.
(9) Rebelo, L. P. N.; Visak, Z. P.; de Sousa, H. C.; Szydlowski, J.; Gomes de Azevedo, R.; Ramos, A. M.; Najdanovic-Visak, V.; Nunes da Ponte, M.; Klein, J. *Macromolecules* **2002**, *35*, 1887.
(10) Zhong, X.; Wang, Y.-X.; Wang, S.-C. *Chem. Eng. Sci.* **1996**, *51*, 3235.
(11) Shibayama, M.; Isono, K.; Okabe, S.; Karino, T.; Nagao, M. *Macromolecules* **2004**, *37*, 2909.
(12) Hirotsu, S.; Hirokawa, Y.; Tanaka, T. *J. Chem. Phys.* **1987**, *87*, 1392.
(13) Shibayama, M.; Tanaka, T.; Han, C. C. *J. Chem. Phys.* **1992**, *97*, 6842.
(14) Shibayama, M.; Tanaka, T.; Han, C. C. *J. Phys. IV* **1993**, *Colloque C8*, 25.
(15) Borue, V.; Erukhimovich, I. *Macromolecules* **1988**, *21*, 3240.
(16) Joanny, J. F.; Leibler, L. *J. Phys. (Paris)* **1991**, *51*, 545.
(17) Provencher, S. W. *Comput. Phys. Comm.* **1982**, *27*, 213.
(18) Pusey, P. N.; van Megen, W. *Physica A* **1989**, *157*, 705.
(19) Panyukov, S.; Rabin, Y. *Phys. Rep.* **1996**, *269*, 1.
(20) Kunugi, S.; Takano, K.; Tanaka, N. *Macromolecules* **1997**, *30*, 4499.
(21) Sawamura, S.; Kitamura, K.; Taniguchi, Y. *J. Phys. Chem.* **1989**, *93*, 4931.
(22) Shibayama, M.; Mizutani, S.; Nomura, S. *Macromolecules* **1996**, *29*, 2019.
(23) Otake, K.; Karaki, R.; Ebina, T.; Yokoyama, C.; Takahashi, S. *Macromolecules* **1993**, *26*, 2194.
(24) Hecht, A. M.; Duplessix, R.; Geissler, E. *Macromolecules* **1985**, *18*, 2167.
(25) Rabin, Y.; Panyukov, S. *Macromolecules* **1997**, *30*, 301.
(26) de Gennes, P. G. *Scaling Concepts in Polymer Physics*; Cornell University: Ithaca, NY, 1979.
(27) Shibayama, M.; Tanaka, T. *J. Chem. Phys.* **1995**, *102*, 9392.
(28) Cho, C. H.; Singh, U. J.; Robinson, G. W. *J. Phys. Chem. B* **1999**, *103*, 1991.
(29) Szydlowski, J.; Rebelo, L. P. N.; Wilczura, H.; Van Hook, W. A.; Melnichenko, Y.; Wignall, G. D. *Fluid Phase Equilib.* **1998**, *150−151*, 687.
(30) Nasimova, I. R.; Karino, T.; Okabe, S.; Nagao, M.; Shibayama, M. *J. Chem. Phys.,* to be submitted.
(31) Schosseler, F.; Skouri, R.; Munch, J. P.; Candau, S. J. *J. Phys. II* **1994**, *4*, 1221.
(32) Ikkai, F.; Shibayama, M.; Han, C. C. *Macromolecules* **1998**, *31*, 3275.
(33) Hirotsu, S. *Phase Transitions* **1994**, *47*, 183.
(34) Shibayama, M.; Tanaka, T.; Han, C. C. *J. Chem. Phys.* **1992**, *97*, 6829.
(35) Porod, G. *Kolloid Z.* **1951**, *124*, 83.
(36) Porod, G. *Kolloid Z.* **1952**, *125*, 51.
(37) Hirokawa, Y.; Jinnai, H.; Nishikawa, Y.; Okamoto, T.; Hashimoto, T. *Macromolecules* **1999**, *32*, 7093.
(38) Philippova, O. E.; Pieper, T. G.; Sitnikova, N. L.; Starodoubtsev, S. G.; Khokhlov, A. R.; Kilian, H. G. *Macromolecules* **1995**, *28*, 3925.
(39) Helgeson, H. C.; Kirkham, D. K. *Am. J. Sci.* **1974**, *274*, 1089.

MA049058E